Evaluation of the potential of *Schinus Terebinthifolius* leaves essential oil as a green inhibitor for E24 steel corrosion in acidic solution

N. Ouadghiri,[1,2]* H.T. Rahal,[3] O. Belhoussaine,[4] A. Chraka,[4] H. Harhar,[5] M. Benmessaoud[1] and S. El hajjaji[2]

[1]*Energy, Materials and Sustainable Development Team, Higher School of Technology Salé, Mohammed V University in Rabat 8007, Morocco*
[2]*Laboratory of Spectroscopy, Molecular Modelling Materials, Nanomaterial Water and Environment–CERNE2D, Faculty of Sciences, Mohammed V University in Rabat, Morocco*
[3]*Department of Chemistry, Faculty of Science, Lebanese International University, Lebanon*
[4]*Laboratory of Materials Engineering and Sustainable Energy (IMED-LAB), Faculty of Science, Abdelmalek Essaadi University, Tetouan, Morocco*
[5]*Materials, Nanotechnology and Environment Laboratory (LMNE), Faculty of Sciences, Mohammed V University of Rabat, BP 1014 Rabat, Morocco*
**E-mail: ouadghirinabil@gmail.com*

Abstract

The inhibitive action of *Schinus Terebinthifolius* Leaves Essential Oil (STLEO) on the corrosion of E24 steel in 1 M HCl solution was investigated using open circuit potential-time measurements (OCP), potentiodynamic polarization (PDP), electrochemical impedance spectroscopy (EIS), and weight loss (WL). Combining EDX assessment with scanning electron microscopy (SEM) allowed for an investigation of the surface morphology of E24 steel. The highest inhibitory efficiencies for the WL, EIS, and PDP methods at 1 g/L of STLEO are 89.33, 85.36, and 88.63%, respectively. It was found that the corrosion inhibition performance depends on the concentration of the studied inhibitor and the solution temperature. Based on Langmuir's isotherm, the tests have demonstrated that STLEO inhibits the corrosion E24 steel in acidic media through a physical adsorption process. The surface morphological observation revealed that the Essential oil forms a barrier that inhibits the transfer of active corrosive species to E24 steel surfaces. Insights from experimental approaches emphasize STLEO's potential as an effective green corrosion inhibitor, offering valuable contributions to practical corrosion protection methods, particularly beneficial for industries relying on E24 steel components in corrosive environments.

Received: June 6, 2024. Published: October 7, 2024 doi: 10.17675/2305-6894-2024-13-4-4

Keywords: *E24 steel, natural extracts, HCl, thermodynamic, adsorption, inhibition.*

1. Introduction

Carbon steel has numerous applications as flow lines, constructions of tanks, and petroleum refinery equipment owing to its simple fabrication process and low cost [1]. However, it undergoes acid pickling or cleaning which results in severe corrosion. Currently, the application of corrosion inhibitors is widely adopted method for safeguarding metals against corrosion. Such inhibitors can significantly decrease the corrosion rate when added to a corrosive environment in small concentrations. Most corrosion inhibitors are organic compounds. Their inhibition property relies on their functional group, which adsorbs on the metal surface. Most of the efficient organic compounds that act as inhibitors have oxygen, sulfur, nitrogen atoms and multiple bonds through which they adsorb on metal surface [2–9]. The creation of a protective barrier film on the metal surface due to these molecules' chemical or physical adsorption may be the cause of the inhibition. Nevertheless, synthetic inhibitors are more expensive than natural inhibitors and require proper selection and dosing to prevent environmental damage and interference with other chemical processes in the system.

Accordingly, efforts are directed towards the use of plant extracts as corrosion inhibitors. Numerous researchers reported the successful use of natural plant extracts on the corrosion inhibition of different metals in aggressive media as they are eco-friendly, cheap, easily obtainable, biodegradable and renewable source for wide range of potential corrosion inhibitors [4, 10–29].

Mamudu and co-workers [30] tested the efficiency of *Dillenia suffruticosa* leaves extract (DSLE) on the corrosion of mild steel in 1 M HCl. DSLE exhibits notable efficacy as a corrosion inhibitor for MS in an acidic environment. The inhibition efficiency (IE) demonstrates a positive correlation with the concentration of the extract, ultimately reaching a maximum value of 81.4% at the optimum concentration of 1000 mg/L of the extract investigated. In a new study, Eddahhaoui *et al.* [31] evaluated the inhibition efficiency of ethanolic extract of *Chamaerops humilis* (CHFE) on the corrosion of low-carbon E24 steel in 1 M HCl solution using the weight loss, potentiodynamic polarization and electrochemical impedance spectroscopy. The results showed that inhibition efficiency increased with increasing with increasing the *C. humilis* extract concentration and reached up to 93% at a concentration of only 500 ppm. Thermodynamic parameters suggest that the adsorption of this extract on the metal surface occurs mainly via physisorption which is inconsistent with Langmuir adsorption isotherm. In the same concept, recently, Zhu *et al.* [32] tested the inhibitive properties of *Zea mays* bracts extract (ZMBE) on the corrosion inhibition of mild steel in 1 M HCl. The results revealed that the corrosion inhibition mechanism of ZMBE for MS is "geometric coverage" effect. The active ingredients in ZMBE can spontaneously adsorb on the MS surface and follow well with the Langmuir isotherm, forming a monolayer adsorption film.

Schinus Terebinthifolius (ST) shrub or small tree that belongs to the Anacardiaceae family, and is native to South America (Brazil, Argentina, Paraguay and Uruguay), generally

colonizing open areas, and is particularly found on forest borders and river margins. This species adapts easily to climate change. It establishes itself through an extensive geographical distribution through plasticity of the species. The wood is used for posts, fuelwood, and charcoal and the plant is also used as a feed supplement for animals. It is also used to obtain essential oils and resins, which are used in leather tanning, pharmaceuticals, cosmetics, the perfumery industry, or the strengthening of fishing nets. Besides, the fruits are highly appreciated as a condiment in foreign cooking, mainly in Europe, where it is used as a spice, either alone or in mixtures with pepper. While the fruits of *Schinus Terebinthifolius* are commonly used as spices, the bark, leaves, and roots are traditionally applied in folk medicine [33].

Due to the encouraging results presented by these studies and the continuous research for an affordable and eco-friendly corrosion inhibitor, this research aimed to investigate the effectiveness of *Schinus Terebinthifolius* Leaves Essential Oil (STLEO) as a corrosion inhibitor of E24 steel in acidic solutions. To this end, the anticorrosive properties of STLEO were investigated by gravimetric and electrochemical techniques such as electrochemical impedance spectroscopy and potentiodynamic polarization curves. Scanning electron microscopy (SEM), were also employed to characterize the surface of the metal in order to support the electrochemical techniques.

2. Material and Methods

2.1. Plant material and extraction of essential oil process

The *Schinus Terebinthifolius* Leaves (STL) were collected from Morocco, the region of Rabat (34°01’53.34”) in the month of January–February. To carry out the extraction, the plant leaves were crushed after being dried out of moisture for two weeks.

Using a device similar to a Clevenger, STLEO was extracted using hydrodistillation. Initially, a 2000 mL flask was filled with 200 g of crushed STL at a ratio of 1:3 plant material to water. The flask was heated for six hours until no more essential oil could be extracted. After that, the water and essential oil mixture was dried and put into dark bottles for storage. The yield of essential oil is approximately 0.28%±0.01. Belhoussaine *et al.* [34] reported the same results (0.28%), whereas, Santana *et al.* obtained a lower yield (0.17%) [35].

2.2. Material and Solutions

The study was carried out on E24 steel sheets of chemical composition (wt.%): 0.110% C, 0.240% Si, 0.021% P, 0.16% S, 0.011% Ti, 0.009% Co, 0.077% Cr, 0.47% Mn and 99.046% Fe. The experiments were carried out in a1 M HCl solution by diluting 37% HCl with distilled water. STLEO was added to the blank solution to obtain the desired concentrations (*i.e.*, 0.25, 0.5, 0.75, and 1 g/L) at temperatures ranging from 293 to 323 K.

2.3. Mass loss

Square E24 steel coupons of dimensions 3.0×3.0×0.3 cm^3 were polished with emery paper (600–800–1500–2000), thoroughly washed with distilled water, and lastly dried with acetone then weighed before measurement. Subsequently, they were immersed in 50 ml 1.0 M HCl solutions for 24 hours at 293 K, in the absence and presence of different STLEO concentrations. Submersion was controlled by a water thermostatic bath. Following immersion, the specimens underwent cleaning with water and acetone and were then dried in a desiccator. Analytical balance was used to determine the weight reduction. Each test was repeated three times to verify its reproducibility.

The following formulas were used to calculate the E24 steel's corrosion rates (*CR*) and inhibition efficiency $IE_{CR}(\%)$ based on the measurement of mass loss [36]:

$$CR = \frac{\Delta W}{S \cdot t} \tag{1}$$

$$IE_{CR}(\%) = \frac{CR^0_{corr} - CR^{inh}_{corr}}{CR^0_{corr}} \cdot 100 \tag{2}$$

The immersion time (*t*) is expressed in hours, while the weight loss (*W*) is expressed in grams. Whereas *S* represents the sample's exposed area in cm^2. The corrosion rates in the absence and the presence of the STLEO are represented by CR^0_{corr} and CR^{inh}_{corr}, respectively.

2.4. Electrochemical measurements

Electrochemical tests were achieved in an electrochemical cell of three electrode mode. The working E24 steel electrode (0.78 cm^2), saturated calomel (SCE) as the reference and a platinum foil with a big expose area served as the counter electrode (CE). These studies were conducted using both stationary (PDP) and transient (EIS) approaches. For measurement, every potential was matched to the SCE.

Using a PGZ100 potentiostat, the working electrode was submerged in a 1 M HCl test solution for thirty minutes, or until the steady state corrosion potential (E_{corr}) was attained. Polarization curve measurements were obtained at a scan rate of 1 mV/min starting from cathodic potential (E_{corr}=–00 mV) going to anodic direction (E_{corr}=–100 mV). The frequency range for electrochemical impedance spectroscopy (EIS) measurements was 100 kHz to 0.01 Hz with applied potential signal amplitude of ±10 mV around the rest potential.

The inhibitory efficacy of the test chemical was calculated by employing the subsequent formulas [37, 38].

$$IE(\%) = \frac{i^0_{corr} - i^{inh}_{corr}}{i^0_{corr}} \cdot 100 \tag{3}$$

where i^0_{corr} and i^{inh}_{corr} represents the corrosion current density without and with STLEO, respectively.

$$IE(\%) = \frac{R_{ct}^{inh} - R_{ct}^{0}}{R_{ct}^{inh}} \cdot 100 \quad (4)$$

where R_{ct}^{inh} and R_{ct}^{0} are the values of the charge transfer resistance (Ω cm^2) obtained from EIS measurements fitting data to an electrical equivalent circuit in the absence and presence and absence of STLEO, respectively.

2.5. Surface analysis by scanning electron microscopy

Scanning Electron Microscopy (SEM) was employed to characterize the surface morphology of E24 steel samples in the absence and presence of STLEO with JOEL Quanta 200 FEI Company scanning electron microscope. The accelerating beam's 20 kV energy is put to use. The equipment has a backscattered electron detector and a complete X-ray microanalysis apparatus (EDS detector).

3. Results and Discussion

3.1. Gas chromatography–mass spectroscopy analysis

The active compounds present in STLEO with their retention times are displayed in Table 1. Thirty-one compounds were identified in STLEO. The results revealed that Limonene (23.22%), followed by Spathulenol (14.34%), β-ocimene (13.32%), γ-terpinene (9.45%) and Sabinol (5.07%) are present as the major components of this oil. Belhousaine *et al.* [34] has found the same results, with limonene as major compounds. The later was found to have a good inhibitory effect in the work of Bensabah *et al.* [39], in other works limonene was used to improve the corrosion resistance of epoxy coatings [40].

The major compounds are also indicative of the antioxidant and anti-bacterial activities of STLEO. The bioactivity of leaf extracts is attributed to phytochemical constituents. Numerous chemical substances, including phenolic compounds, sesquiterpene hydrocarbons, monoterpene hydrocarbons, oxygenated monoterpenes, and oxygenated sesquiterpene, are present in the STLEO [34, 35, 41–43].

Generally, the chemical makeup of STLEO varies according to the section of the plant being extracted, the extraction methods, and the surrounding environment.

Table 1. Chemical composition of the STLEO.

Retention time	Name of detected compound	Formula	%
11.47	β-ocimene	$C_{10}H_{16}$	13.32
11.64	Camphene	$C_{10}H_{16}$	0.91
12.02	β-phellandrene	$C_{10}H_{16}$	0.96
12.13	β-pinene	$C_{10}H_{16}$	1.48
12.33	β-myrcene	$C_{10}H_{16}$	4.22

Retention time	Name of detected compound	Formula	%
12.74	γ-terpinene	$C_{10}H_{16}$	9.45
13.13	Limonene	$C_{10}H_{16}$	23.22
13.98	Terpinolene	$C_{10}H_{16}$	2.09
14.53	*p*-menth-2-en-1-ol	$C_{10}H_{18}O$	0.62
14.60	α-campholenal	$C_{10}H_{16}O$	0.20
14.89	Pinocarvéol	$C_{10}H_{16}O$	0.40
14.99	Verbenol	$C_{10}H_{16}O$	0.28
15.30	Carvenone	$C_{10}H_{16}O$	1.26
15.42	Terpinen-4-ol	$C_{10}H_{18}O$	0.37
15.49	*p*-cymen-8-ol	$C_{10}H_{14}O$	0.77
15.84	Sabinol	$C_{10}H_{16}O$	5.07
16.41	Carvone	$C_{10}H_{14}O$	0.27
16.60	Piperitone	$C_{10}H_{16}O$	0.35
16.92	Phellandral	$C_{10}H_{16}O$	0.42
17.08	Thymol	$C_{10}H_{14}O$	1.75
17.62	Caryophyllene oxide	$C_{15}H_{24}O$	0.28
17.71	Citronellol acetate	$C_{12}H_{22}O_2$	2.25
17.86	Géranyl acetate	$C_{12}H_{20}O_2$	0.50
18.33	β-gurjunene	$C_{15}H_{24}$	0.53
18.53	β-elemene	$C_{15}H_{24}$	0.26
18.95	Caryophyllene	$C_{15}H_{24}$	0.41
19.25	Alloaromadendrene	$C_{15}H_{24}$	0.66
19.76	Germacrene D	$C_{15}H_{24}$	2.00
20.00	γ-elemene	$C_{15}H_{24}$	0.42
20.22	δ-cadinene	$C_{15}H_{24}$	0.35
21.04	Spathulenol	$C_{15}H_{24}O$	14.34

3.2. Weight loss measurements

Weight loss measurements were conducted to assess the impact of inhibitor concentrations on the corrosion inhibition of E24 steel in a 1 M HCl solution after 24 h. Figure 1 illustrates the corrosion rate and inhibition effectiveness as a function of different inhibitor concentrations (0.25 to 1.0 g/L) [44, 45].

It is clearly observed that the corrosion rate of E24 steel is significantly reduced with increasing STLEO concentration. This reduction in corrosion rate is attributed to the adsorption of the STLEO inhibitor onto the steel surface, forming a protective layer that hinders the access of aggressive ions to the metal surface [46]. The inhibition efficiency was found to be particularly high, reaching 96.1% in a 1 M HCl solution containing 1 g/L of STLEO. This achievement demonstrated the potential of STLEO as an effective corrosion inhibitor [47].

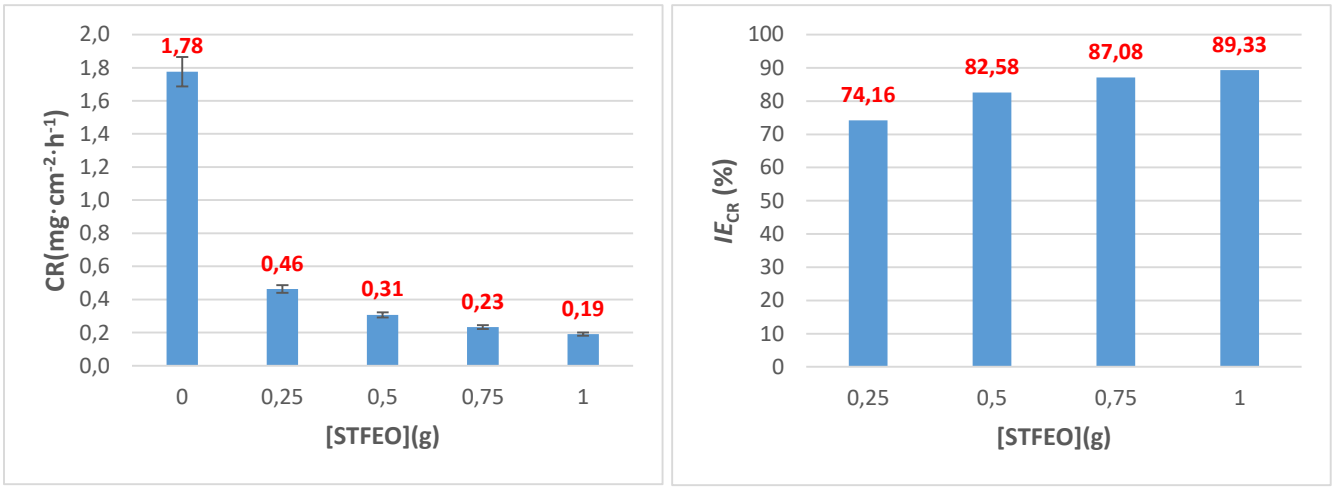

(a) (b)

Figure 1. Evaluation of Corrosion Rate *CR* and Inhibition Efficiencies IE_{CR} (%) with different concentrations of STLEO after 24 hours of immersion time at 293 K for E24 steel in 1 M HCl.

3.3. Polarization results

3.3.1. Open Circuit Potential measurements (OCP)

OCP is an essential technique that enables the determination of the corrosion behavior. Figure 2 shows that the OCP of E24 steel was shifted to less negative values in the presence of STLEO. Such positive shift indicates the influence of STLEO on the dissolution process of E24 steel occurring at anodic sites. An inhibitor can be categorized as either cathodic or anodic when the change in the corrosion potential (E_{corr}) value is more than 85 mV. Thus, STLEO can be considered a mixed-type inhibitor of E24 steel in 1 M HCl solutions because its highest displacement is about 60 mV [11].

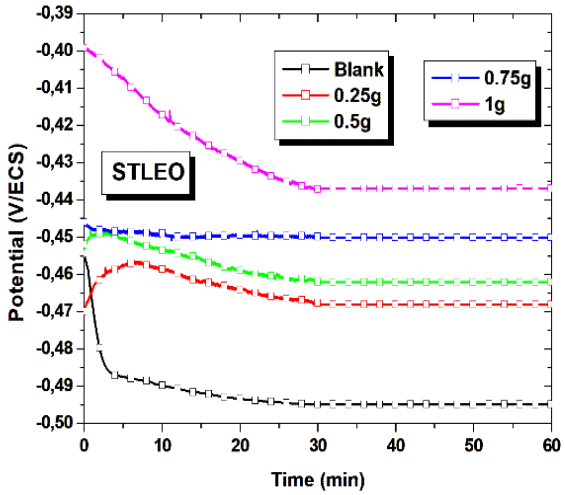

Figure 2. Evolution of the OCP as a function of exposure time of E24 steel in a 1 M HCl solution without and with various concentrations of STLEO at 293 K.

3.3.2. Concentration effect

The potentiodynamic polarization curves for E24 steel in 1 M HCl in the absence and presence of various concentrations of STLEO at 293 K are depicted in Figure 3. It is clearly observed that the addition of STLEO suppresses both anodic and cathodic parts of the polarization curves indicating it acts as mixed-type inhibitor for E24 steel corrosion in 1 M HCl. Moreover, it is noted that the addition of STLEO shifts the corrosion potential of mild steel to more positive values.

The electrochemical parameters: corrosion potential, E_{corr}; anodic and cathodic Tafel slopes, β_a, β_c; and corrosion current density (i_{corr}), obtained from these curves together with the percentage of inhibition efficiency (%P) are given in Table 1.

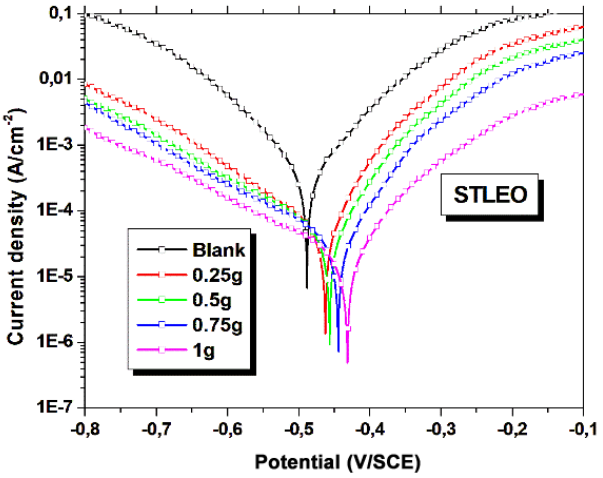

Figure 3. Potentiodynamic polarization curves for E24 steel in 1 M HCl without and with various concentrations of STLEO at 293 K.

Table 2. The electrochemical polarization characteristics for the corrosion of E24 steel in 1 M HCl without and with various concentrations of STLEO at 293 K.

[STLEO] g/L	E_{corr} mV/SCE	i_{corr} μA/cm^2	β_c mV/dec	β_a mV/dec	*IE*, %
0	–488±1.4	174.8±1.11	–94.7±2.4	93.3±3.1	–
0.25	–462±0.5	49.5±0.97	–140.3±2.9	54.2±1.1	72.32
0.5	–456±0.6	32.2±1.39	–143.4±3.9	61.1±1.4	81.56
0.75	–444±0.8	25.1±0.99	–157.6±4.8	64.4±0.9	85.93
1	–431±1.1	19.9±0.81	–201.5±8.1	81.9±1.3	88.63

The tabulated data revealed that corrosion current density (i_{corr}) decreases from 174.8 to 19.9 μA·cm^{-2} with increasing STLEO concentrations accompanied with an increase in %P to reach 88.63% at a concentration of 1 g/L. The slight variations in anodic Tafel slopes and cathodic Tafel slopes (β_a and β_c), in the presence STLEO, indicates that the inhibiting action is taking place by simple blocking of the available anodic and cathodic sites on the metal surface [41]. The β_c and β_a are given in these formulas, $\beta_c = 2.303RT/\alpha nF$ and $\beta_a = 2.303RT/(1-\alpha)nF$ where R is the gas constant, 8.314 Joule/mol·K; T is the absolute temperature, α is the "symmetry factor" nominally 0.5, $F = 96540$ C/mol is Faraday's constant; and n is the number of electrons transferred in the rate determining step. As seen, values of β_a are generally smaller β_c than and are about 60 mV indicating exchange of two electrons during metal dissolution process [42]. Moreover, the change in the E_{corr} value observed in Table 1 does not exceed 85 mV, it can be concluded that the inhibitor under examination exhibits a mixed nature.

3.3.3. Temperature effect

In order to examine the effect of temperature on STLEO's inhibitory efficacy, the optimal concentration (1 g/L) was used at temperatures ranging from 293 to 323 K. The PDP curves obtained in 1 M HCl, both in the absence and presence of 1 g/L of STLEO at various temperatures, are displayed in Figure 4. Table 3 shows the electrochemical parameters obtained by extrapolating the Tafel lines from the polarization curves.

The obtained results reveal that the corrosion rate increases at elevated temperatures for both blank and inhibited solutions as well as the inhibition efficiency of STLEO decreases upon increasing temperature. This may be attributed to many factors such as the degradation of the inhibitor's structure or a weakening of the attraction forces responsible for the adsorption phenomenon.

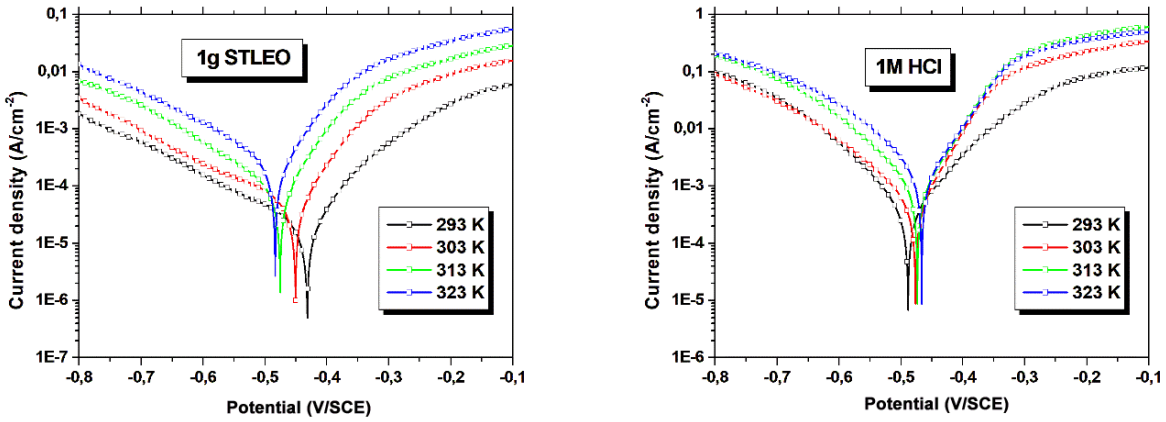

Figure 4. Polarization curves relating to the behavior of E24 steel at different temperatures in the absence and presence of 1 g/L STLEO

Table 3. Change in E24 steel's electrochemical characteristics with temperature in the absence and presence of 1 g/L STLEO.

***T*, K**	**Inhibitor**	***E*corr, mV/SCE**	***i*corr, μA/cm^2**	***IE*, %**
293	Blank	–488±1.4	174.8±1.11	–
	STLEO	–431 ± 1.1	19.9 ± 0.81	88.63
303	Blank	–476±1.6	234.7±2.38	–
	STLEO	–451 ± 0.9	38.1±1.10	83.77
313	Blank	–473 ± 2.1	341.7±2.95	–
	STLEO	–475 ± 1.3	80 ± 0.90	80.56
323	Blank	–466 ± 0.9	735.6 ± 3.15	–
	STLEO	–483±2.1	199.2±2.65	72.92

The activation and thermodynamic parameters are of great importance for elucidating the mechanism of corrosion inhibition of different metals. The activation and thermodynamic parameters (apparent activation energy (E_a), enthalpy (ΔH_a) and entropy (ΔS_a)) for E24 steel in 1 M HCl in the absence and presence of 1 g·L^{-1} STLEO extract were obtained from the Arrhenius and transition state plots shown in Figure 5 according to the following equations [36]:

$$\ln\left(i_{corr}\right) = -\frac{E_a}{RT} + \ln A \qquad (5)$$

$$i_{corr} = \frac{RT}{Nh}\exp\left(\frac{\Delta S_a}{R}\right)\exp\left(-\frac{\Delta H_a}{RT}\right) \quad (6)$$

where R is the gas constant, T is the absolute temperature, A is the Arrhenius pre-exponential factor, N is the Avogadro number, and h is the Plank constant.

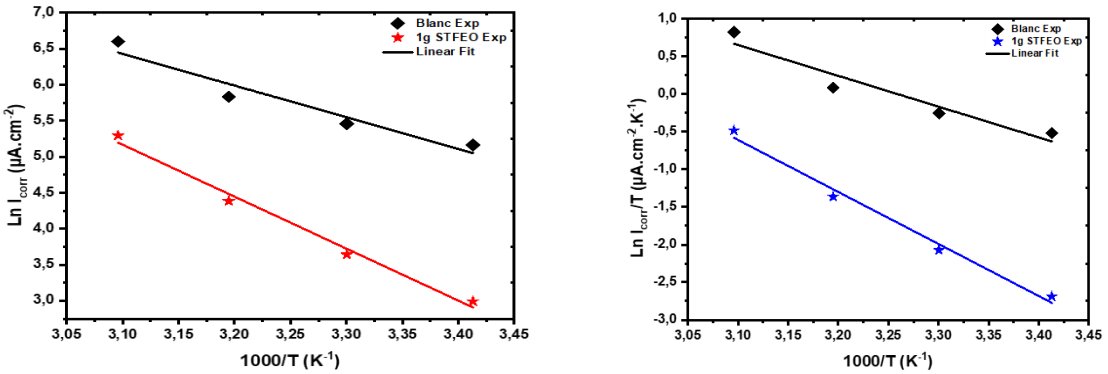

Figure 5. Arrhenius (a) and ln (i_{corr}/T) (b) plots as a function of 1000/T in a 1 M HCl solution without and with 1 g/L of STLEO at various temperatures.

The calculated parameters for solutions containing 1 g/L of STLEO and the corresponding blank solution are given in Table 4.

Table 4. Activation parameters for the E24 steel dissolution in 1 M HCl without and with 1 g/L STLEO.

	E_a kJ mol^{-1}	ΔH_a kJ mol^{-1}	ΔS_a kJ mol^{-1}	$E_a - \Delta H_a$
Blank	36.61	34.05	–86.53	2.56
1 g STLEO	60.04	57.48	–24.39	2.56

As shown in Table 4, the E_a for the inhibited solutions (60.04 kJ·mol^{-1}) is higher than the blank solution (36.61 kJ·mol^{-1}). Due to the formation of a protective film, the inhibitor with a higher E_a introduces greater energy barriers to the corrosion process and to the dissolution of metals [48]. The values of ΔH_a reported in Table 5 are close to E_a and positive. This illustrates the endothermic nature of the dissolution of the steel in the 1.0 M HCl solution. [49]. In another way, standard entropy (ΔS_a), which describes the system's randomness, increases in the presence of inhibitors, implying a spontaneous reaction.

3.4. Electrochemical impedance spectroscopy (EIS)

Electrochemical impedance spectroscopy (EIS) is an influential non-destructive method used to investigate electrochemical systems. It is being broadly applied in the corrosion and electrochemistry fields to study the corrosion inhibition of different compounds and predict the corrosion rates of different metals. Figure 6 reveals that the Nyquist impedance plots for

E24 steel after 1 hour of exposure to 1 M HCl in the absence and presence of STLEO consist of depressed capacitive semicircle signifying that the dissolution process of E24 steel occurs under activation control. The depressed capacitive loop is ascribed to dispersion effects, which have been attributed to roughness and inhomogeneities on the surface during corrosion [50].

The Bode modulus plots demonstrate that the impedance increases gradually with increases in concentration, indicating a higher inhibition efficiency of STLEO. The phase angle value increased significantly with increasing inhibitor concentration. It was noted that the phase angle values were always higher in the presence of STLEO compared to the blank, but lower than −90, indicating the non-ideal capacitor [51]. The spectra obtained showed show a one-time constant, which is attributed to the electrical double layer [52].

The electrochemical impedance parameters achieved by fitting the impedance curves to a simple equivalent circuit model (Figure 6) which includes the solution resistance R_s and the constant phase element (CPE) which is employed to analyze the data collected from the impedance in place of a pure capacitor due to the non-ideal behavior of the metal surface. The CPE is placed in parallel to charge transfer resistance element, R_{ct}. The R_{ct} value is a measure of electron transfer across the surface and is inversely proportional to corrosion rate.

Nyquist impedance plots were analyzed using Z-view software.

Table 5 displays the obtained impedance parameters. Equation 4 was used to calculate the inhibition efficiency for electrochemical impedance spectroscopy curves.

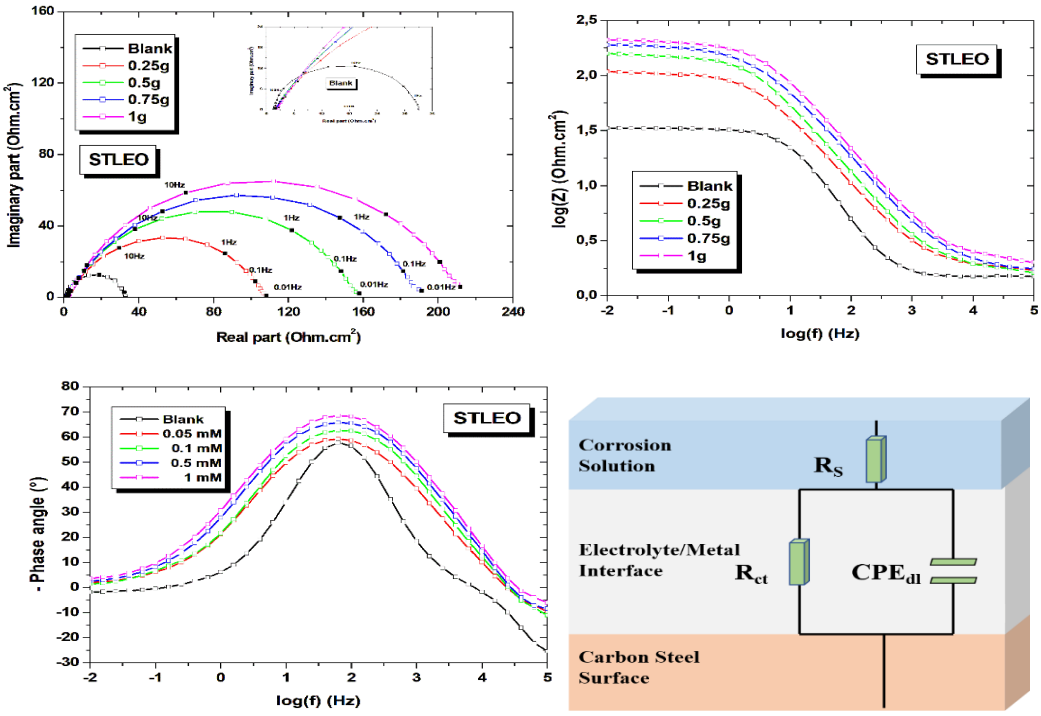

Figure 6. Nyquist, Bode modulus, Phase angle plots and Equivalent Electric Circuit of E24 steel in 1 M HCl solution in the absence and presence of different concentrations of STLEO at 293 K.

The tabulated data revealed that, in contrast to the values of C_{dl}, which showed a considerable drop, the addition of STLEO constantly boosted the charge transfer resistance values, which increased with increasing inhibitor concentration. This may be attributed to the adsorption of a sizable number of molecules on the surface of E24 steel, which modified the metal/electrolyte interface by causing an important rise in the double electric layer thickness.

Table 5. EIS data recorded for E24 steel in 1 M in the absence and presence of different concentrations of STLEO at 293 K.

[STLEO] g/L	R_s **Ω·cm²**	R_{ct} **Ω·cm²**	CPE_{dl} **μF·cm⁻²**	***n***	***EI*** **%**	**θ**
0	1.92±0.45	31.14±1.35	511.1±3.25	0.725±0.002	–	–
0.25	1.86±0.40	108.3±0.98	92.8±2.01	0.723±0.003	71.25	0.7125
0.5	2.39±0.27	153.0±1.25	65.7±1.95	0.725±0.004	79.65	0.7965
0.75	2.07±0.17	187.5±2.19	53.4±1.48	0.708±0.003	83.39	0.8339
1	4.23±0.29	212.7±3.81	47.3±0.98	0.734±0.005	85.36	0.8536

3.5. Adsorption isotherm

Adsorption of molecules on the metal surfaces plays an important role in inhibition of corrosion. The adsorption isotherm can give fundamental details about how the inhibitor interacts with the E24 steel surface [53]. Thus, Langmuir isotherm has been tested to adapt the surface coverage degree (θ) obtained for STLEO. It was found that the plot C_{inh}/θ against C_{inh} (Figure 7) gives a straight line with a correlation coefficient of 0.999 providing that the adsorption of STLEO on the E24 steel surface obeys the Langmuir adsorption isotherm. This isotherm can be represented by [54]:

$$\frac{C_{inh}}{\theta} = \frac{1}{k_{ads}} + C_{inh} \tag{7}$$

C_{inh} represents the inhibitor concentration, while k_{ads} is the adsorption process's equilibrium constant which is linked to the free energy of the adsorption (ΔG_{ads}) according to the following equation [45, 51]:

$$\Delta G_{ads} = -RT \ln\left(55.5 k_{ads}\right) \tag{8}$$

where R is the molar gas constant, T is the absolute temperature in Kelvin and 55.5 is the molar concentration of water in solution.

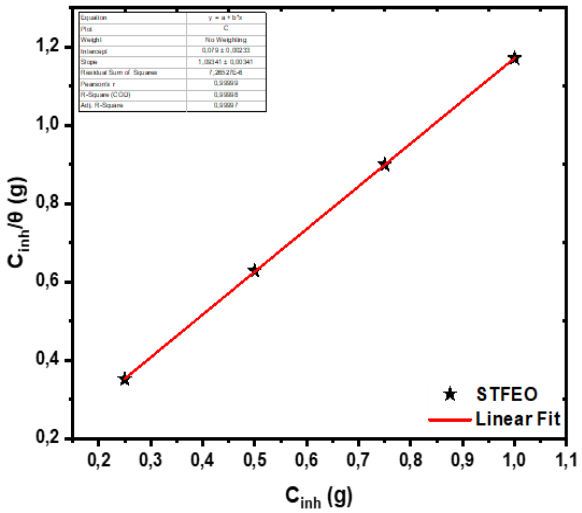

Figure 7. Langmuir's isotherm adsorption model of STLEO on the E24 steel surface in 1 M HCl at 293 K.

Table 6. Calculated adsorption parameters for the adsorption of STLEO on E24 steel surface.

Inhibitor	***K*, mol^{-1}·L**	***R*^{2}**	**ΔG^0_{ads}, kJ·mol^{-1}**
STLEO	12.65	0.99	–15.96

As seen from Table 6, the negative value of ΔG^0_{ads} reflects the spontaneity of the adsorption process of STLEO and the stability of the adsorbed layers on the E24 steel surface in 1 M HCl solutions. Usually, values of ΔG_{ads} up to –20 kJ·mol^{-1} indicate an electrostatic interaction between the charged molecules and the metal (physical adsorption) [10, 13, 50]. Therefore, it could be concluded that STLEO inhibits the corrosion of E24 steel in acidic media through physical adsorption mechanism [55]. Physical adsorption is typically achieved through electrostatic attraction between charged metal surfaces and charged organic substances [56]. It can also be facilitated through dispersion and induction forces related to the polar functional groups in organic molecules. So, the behavior of STLEO may be probably due to the adsorption of cationic moieties of the extracted molecules, π-electrons, free lone-pair nitrogen and oxygen heteroatoms electrons and other polar groups present in STLEO over the E24 steel surface. Conversely, due to the low electron-donating ability of cations, the tendency to chemical adsorption is very weak which supports the physical adsorption mechanism of STLEO on E24 steel surface in the acidic environment [1, 12, 57].

4. SEM observation

Figure 8 shows the E24 steel's surface state as observed by SEM analysis following a 24 hour immersion in a 1 M HCl solution (a) and 1 g/L of STLEO (b). The E24 steel surface seems rough damaged and severely corroded due to the aggressive attack of 1 M HCl in 12 (a). On the other hand, in 12 (b), the corrosion activity was suppressed as seen from the decrease in localized corrosion areas and the metal coupons appeared smooth. This is due to the adsorption of the STLEO on the steel surface forming a protective barrier against corrosion activity.

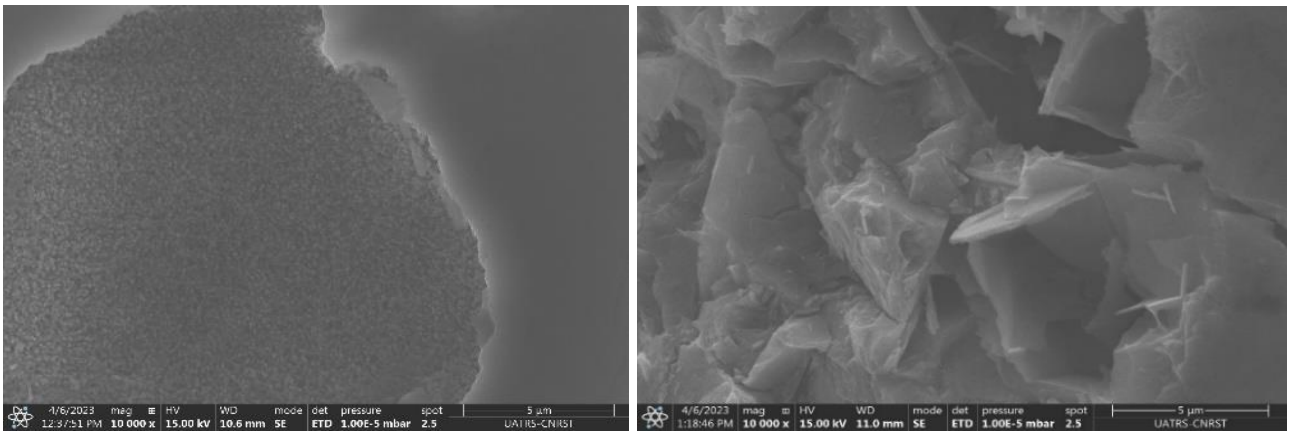

(a) (b)

Figure 8. Micrographs showing of E24 in without inhibitor (a) and with 1 g STLEO (b) after 24 hours of immersion in 1.0 M HCl solution.

Furthermore, to identify the elemental composition of E24 steel samples before and after the addition of STLEO, EDX analysis was performed and analyzed. Figure 9 shows the EDX spectra of E24 steel in the absence and presence of 1 g/L of STLEO in 1.0 M HCl solution after 24 hours of immersion. For the blank solution, the presence of oxygen and iron atoms suggests the presence of corrosion products composed of iron hydroxide and/or oxide (Figure 9a). However, the oxygen peak is much larger in the presence of STLEO (Figure 9b), which is certainly due to the adsorption of active ingredients of STLEO on the metallic surface. The presence of Cl atom suggested that the formed film by STLEO blocks the attack by chloride ions, which accumulate on the film surface.

These findings are in quite good agreement with the results obtained previously from electrochemical measurements. They confirm the adsorption of STLEO on E24 steel surface and the formation of a protective layer from corrosive ions.

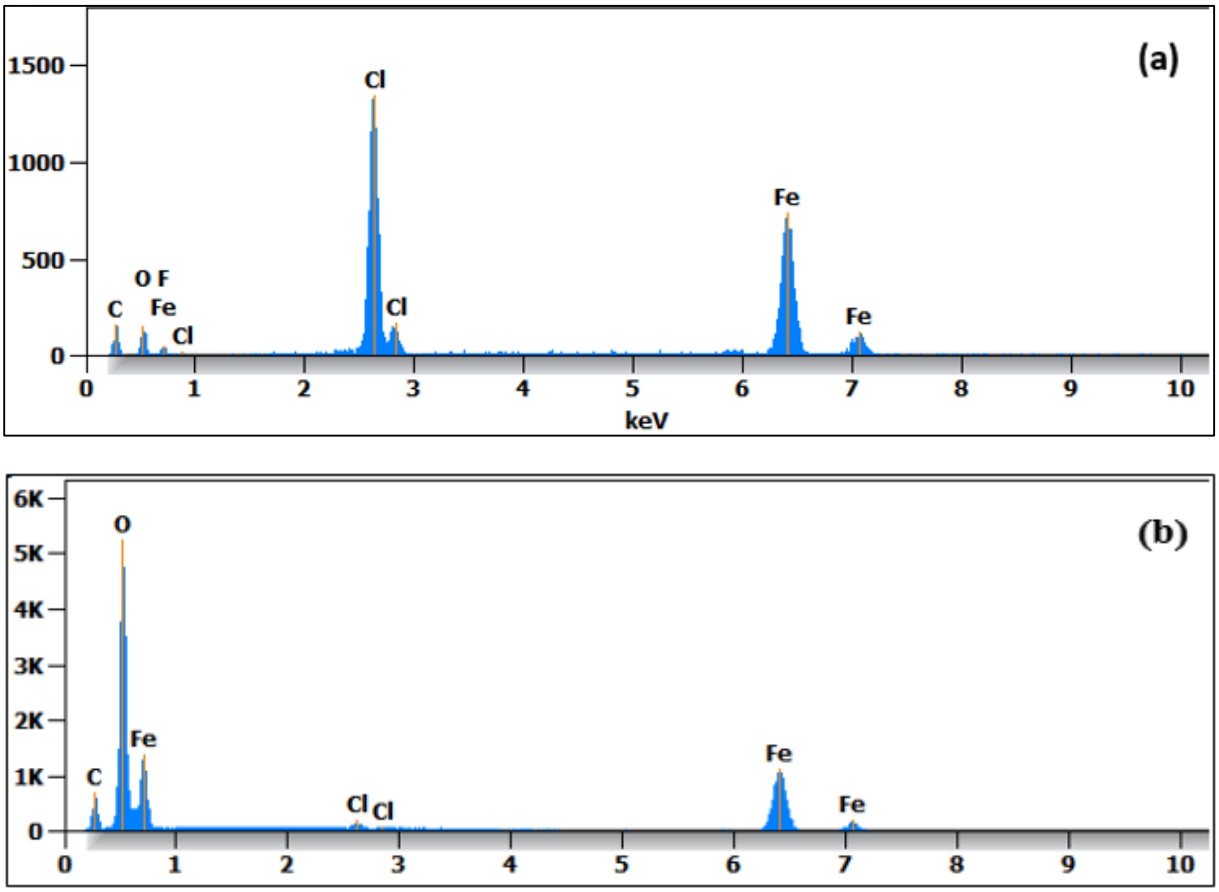

Figure 9. EDX spectra of E24 steel without inhibitor (a) and with inhibitor 1 g/L of STLEO (b) in 1.0 M HCl solution after 24 hours of immersion.

5. Conclusion

Our findings indicate that *Schinus Terebinthifolius* leaf essential oil is a potent corrosion inhibitor for E24 steel in 1 M hydrochloric acid medium that is both effective, of natural origin and environmentally friendly. The inhibitory efficacy obtained increases with concentration, reaching 88.63% at 1 g/L, and decreases with increasing temperature. The curves indicate that our extract acts mainly as a mixed-type inhibitor with predominantly anodic action.

EIS results show that the addition of STLEO leads to a decrease in C_{dl} value and an increase in R_{ct} values and thus a reduction in CR corrosion rate, indicating that our inhibitor is adsorbed at the metal-electrolyte interface, and the circuit model matches the data obtained and an analogous model has a constant phase element.

The negative value of ΔG^0_{ads} confirms the spontaneous nature of the adsorption process and the stability of the adsorbed double layer on the metal surface, while its absolute value underlines that the interactions between the inhibitor and the metal surface are physical, indicating mixed adsorption.

The adsorption of STLEO molecules follows the Langmuir adsorption isotherm model. In addition, SEM/EDX examination confirms the presence of a protective protective adsorbed film deposited on the metal surface.

These conclusions are made more reliable by the consistency observed in the gravimetric, EIS and potentiodynamic polarization results.

References

1. H.T. Rahal, A.M. Abdel-Gaber and G.O. Younes, Inhibition of steel corrosion in nitric acid by sulfur containing compounds, *Chem. Eng. Commun*., 2016, **203**, 435–445. doi: 10.1080/00986445.2015.1017636
2. O.O. Fadare, A.E. Okoronkwo and E.F. Olasehinde, Assessment of anti-corrosion potentials of extract of *Ficus asperifolia-Miq* (*Moraceae*) on mild steel in acidic medium, *Afr. J. Pure Appl. Chem*., 2024, **10**, 8–22. doi: 10.5897/AJPAC2015.0651
3. M. Pourmohseni, A. Rashidi and M. Karimkhani, Preparation of corrosion inhibitor from natural plant for mild stil immersed in an acidic environmental: experimental and theoretical study, *Sci. Rep*., 2024, **14**, 7937. doi: 10.1038/s41598-024-58637-z
4. H.T. Rahal, A.M. Abdel-Gaber, R. Al-Oweini and R.N. El-Tabesh, Corrosion inhibition and adsorption properties of some manganese metal complexes on mild steel in sulfuric acid solutions, *Int. J. Corros. Scale Inhib*., 2024, **13**, no. 2, 708–726. doi: 10.17675/2305-6894-2024-13-2-4
5. A.J.M. Eltmimi, A. Alamiery, A.J. Allami, R.M. Yusop, A.H. Kadhum and T. Allami, Inhibitive effects of a novel efficient Schiff base on mild steel in hydrochloric acid environment, *Int. J. Corros. Scale Inhib*., 2021, **10**, no. 2, 634–648. doi: 10.17675/2305-6894-2021-10-2-10
6. M. Abouchane, R. Hsissou, A. Chraka, A. Molhi, M. Damej, K. Tassaoui, A. Berisha, M. Seydou, B.O. Elemine and M. Benmessaoud, Synthesis and characterization of new macromolecular epoxy resin as an effective corrosion inhibitor for C38 steel in 1 M HCl medium: electrochemical insights, surface morphological and computational approaches, *J. Bio Tribo Corros*., 2024, **10**, 21. doi: 10.1007/s40735-024-00824-6
7. M. Abouchane, R. Hsissou, A. Molhi, M. Damej, K. Tassaoui, A. Berisha, A. Chraka and M. Benmessaoud, Exploratory experiments supported by modeling approaches for TGEEA new epoxy resin as a contemporary anti-corrosion material for C38 steel in 1.0 M HCl, *J. Fail. Anal. Prev*., 2023, **23**, 1765–1781. doi: 10.1007/s11668-023-01705-9
8. Z. Lakbaibi, M. Damej, A. Molhi, M. Benmessaoud, S. Tighadouini, A. Jaafar, T. Benabbouha, A. Ansari, A. Driouich and M. Tabyaoui, Evaluation of inhibitive corrosion potential of symmetrical hydrazine derivatives containing nitrophenyl moiety in 1 M HCl for C38 steel: experimental and theoretical studies, *Heliyon*, 2022, **8**. doi: 10.1016/j.heliyon.2022.e09087

9. M. Damej, A. Molhi, K. Tassaoui, B. El Ibrahimi, Z. Akounach, A.A. Addi, S. El Hajjaji and M. Benmessaoud, Experimental and Theoretical Study to Understand the Adsorption Process of p-Anisidine and 4-Nitroaniline for the Dissolution of C38 Carbon Steel in 1 M HCl, *ChemistrySelect*, 2022, **7**. doi: 10.1002/slct.202103192
10. R.S. Al-Moghrabi, A.M. Abdel-Gaber and H.T. Rahal, Corrosion inhibition of mild steel in hydrochloric and nitric acid solutions using willow leaf extract, *Prot. Met. Phys. Chem. Surf*., 2019, **55**, 603–607. doi: 10.1134/s2070205119030031
11. L.W. El Khatib, H.T. Rahal and A.M. Abdel-Gaber, Synergistic effect between *Fragaria ananassa* and *Cucurbita pepo L* leaf extracts on mild steel corrosion in hydrochloric acid solutions, *Prot. Met. Phys. Chem. Surf*., 2020, **56**, 1096–1106. doi: 10.1134/S2070205120050111
12. M. Kilo, H.T. Rahal, M.H. El-Dakdouki and A.M. Abdel-Gaber, Study of the corrosion and inhibition mechanism for carbon steel and zinc alloys by an eco-friendly inhibitor in acidic solution, *Chem. Eng. Commun*., 2021, **208**, 1676–1685. doi: 10.1080/00986445.2020.1811239
13. A.M. Abdel-Gaber, H.T. Rahal and F.T. Beqai, Eucalyptus leaf extract as a eco-friendly corrosion inhibitor for mild steel in sulfuric and phosphoric acid solutions, *Int. J. Ind. Chem*., 2020, **11**, 123–132. doi: 10.1007/s40090-020-00207-z
14. A.M. Abdel-Gaber, H.T. Rahal and M.S. El-Rifai, Green approach towards corrosion inhibition in hydrochloric acid solutions, *Biointerface Res. Appl. Chem*., 2021, **11**, 14185–14195. doi: 10.33263/BRIAC116.1418514195
15. S. El-Housseiny, A.M. Abdel-Gaber, H.T. Rahal and F.T. Beqai, Eco-friendly corrosion inhibitor for mild steel in acidic media, *Int. J. Corros. Scale Inhib*., 2022, **11**, no. 4, 1516–1538. doi: 10.17675/2305-6894-2022-11-4-6
16. G.D. Pai, M.R. Rathod, S.K. Rajappa and A.A. Kittur, Effect of *tabebuia heterophylla* plant leaves extract on corrosion protection of low carbon steel in 1 M HCl medium: Electrochemical, quantum chemical and surface characterization studies, *Res. Surf. Interfaces*, 2024, **15**, 100203. doi: 10.1016/j.rsurfi.2024.100203
17. V.M. Paiva, R. da Silva Nunes, K.C.d.S. de Lima, S.M. de Oliveira, J.R. de Araujo, B.S. Archanjo, A.F. do Valle and E. D'Elia, Novel eco-friendly green inhibitor of corrosion based on acerola (*Malpighia glabra*) waste aqueous extract for mild steel in 1 mol L^{-1} HCl solution, *Surf. Interfaces*, 2024, **47**, 104187. doi: 10.1016/j.surfin.2024.104187
18. S. Sharma, A.S. Solanki and S.K. Sharma, Anticorrosive action of eco-friendly plant extracts on mild steel in different concentrations of hydrochloric acid, *Corros. Rev*., 2024, **42**, 185–201. doi: 10.1515/corrrev-2023-0053
19. A. Berrissoul, A. Dafali, F. Benhiba, H. Outada, I. Warad, B. Dikici and A. Zarrouk, Experimental and theoretical insights into *Artemisia* Stems aqueous extract as a sustainable and eco-friendly corrosion inhibitor for mild steel in 1 M HCl environment, *Environ. Sci. Pollut. Res*., 2024, 1–20. doi: 10.1007/s11356-024-33636-9

20. A.G. Kalkhambkar, S.K. Rajappa and J. Manjanna, Evaluation of *vateria indicia* leaves extract as a green source of potential corrosion inhibitor against mild steel corrosion in 1 M HCl solution: electrochemical, and surface characterisation studies, *Sens. Technol*., 2024, **2**, 2345081. doi: 10.1080/28361466.2024.2345081
21. O. Ninich, E. El Fahime, M. Tiskar, K. Tassaoui, O. Chauiyakh, S. Aarabi, B. Satrani, M. Benmessaoud and A. Ettahir, Cedar tar as a green corrosion inhibitor for E24 steel in 1 M HCl solution: A comparative analysis of uncleaned and cleaned cedar tar, *Int. J. Corros. Scale Inhib*., 2023, **12**, 2142–2170. doi: 10.17675/2305-6894-2023-12-4-38
22. H.A. Al-Sharabi, F. Bouhlal, K. Bouiti, N. Labjar, E. Al Zalaei, A. Dahrouch, G.A. Benabdellah, M. El Mahi, B. Benmessaoud and E.M. Lotfi, Electrochemical and thermodynamic evaluation on corrosion inhibition of C38 steel in 1 M HCl by Rumex ethanolic extract, *Int. J. Corros. Scale Inhib*., 2022, **11**, no. 1, 382–401. doi: 10.17675/2305-6894-2022-11-1-23
23. Z. Akounach, A. Al Maofari, A. El Yadini, S. Douche, M. Benmessaoud, B. Ouaki, M. Damej and S.E.L. Hajjaji, Inhibition of mild steel corrosion in 1.0 M HCl by water, hexane and ethanol extracts of *pimpinella anisum* plant, *Anal. Bioanal. Electrochem*., 2018, **10**, 1506.
24. A.I. Ikeuba and P.C. Okafor, Green corrosion protection for mild steel in acidic media: saponins and crude extracts of *Gongronema latifolium*, *Pigm. Resin Technol*., 2019, **48**, 57–64. doi: 10.1108/PRT-03-2018-0020
25. R. Haldhar, D. Prasad and N. Bhardwaj, Extraction and experimental studies of *Citrus aurantifolia* as an economical and green corrosion inhibitor for mild steel in acidic media, *J. Adhes. Sci. Technol*., 2019, **33**, 1169–1183. doi: 10.1080/01694243.2019.1585030
26. P. Mourya, S. Banerjee and M.M. Singh, Corrosion inhibition of mild steel in acidic solution by *Tagetes erecta* (Marigold flower) extract as a green inhibitor, *Corros. Sci*., 2014, **85**, 352–363. doi: 10.1016/j.corsci.2014.04.036
27. T.K. Bhuvaneswari, V.S. Vasantha and C. Jeyaprabha, *Pongamia pinnata* as a green corrosion inhibitor for mild steel in 1N sulfuric acid medium, *Silicon*, 2018, **10**, 1793–1807. doi: 10.1007/s12633-017-9673-3
28. P. Tiwari, M. Srivastava, R. Mishra, G. Ji and R. Prakash, Economic use of waste *Musa paradisica* peels for effective control of mild steel loss in aggressive acid solutions, *J. Environ. Chem. Eng*., 2018, **6**, 4773–4783. doi: 10.1016/j.jece.2018.07.016
29. K. Boumhara, H. Harhar, M. Tabyaoui, A. Bellaouchou, A. Guenbour and A. Zarrouk, Corrosion inhibition of mild steel in 0.5 M H_2SO_4 solution by *artemisia herba-alba* oil, *J. Bio Tribo Corros*., 2019, **5**, 1–9. doi: 10.1007/s40735-018-0202-8
30. U. Mamudu, J.H. Santos, S.A. Umoren, M.S. Alnarabiji and R.C. Lim, Investigations of corrosion inhibition of ethanolic extract of *Dillenia suffruticosa* leaves as a green corrosion inhibitor of mild steel in hydrochloric acid medium, *Corros. Commun*., 2024, **15**, 52–62. doi: 10.1016/j.corcom.2023.10.005

31. F.-Z. Eddahhaoui, A. Najem, M. Elhawary, M. Boudalia, O.S. Campos, M. Tabyaoui, A.J. Garcia, A. Bellaouchou and H.M.A. Amin, Experimental and computational aspects of green corrosion inhibition for low carbon steel in HCl environment using extract of *Chamaerops humilis* fruit waste, *J. Alloys Compd*., 2024, **977**, 173307. doi: 10.1016/j.jallcom.2023.173307
32. J.-h. Zhu, B.-l. Lin, T.-h. Duan, H.-q. Lin, G.-y. Zhang, X.-x. Zhou and Y.-y. Xu, Zea mays bracts extract as an eco-friendly corrosion inhibitor for steel in HCl pickling solution: Experimental and simulation studies, *Arabian J. Chem*., 2024, **17**, 105895. doi: 10.1016/j.arabjc.2024.105895
33. E.C. Rosas, L.B. Correa and M. das Graças Henriques, Antiinflammatory properties of *Schinus Terebinthifolius* and its use in arthritic conditions, in: *Bioactive food as dietary interventions for arthritis and related inflammatory diseases*, Elsevier, 2019, pp. 489–505. doi: 10.1016/B978-0-12-813820-5.00028-3
34. O. Belhoussaine, C. El Kourchi, H. Harhar, A. Bouyahya, A. El Yadini, F. Fozia, A. Alotaibi, R. Ullah and M. Tabyaoui, Chemical composition, antioxidant, insecticidal activity, and comparative analysis of essential oils of leaves and fruits of *Schinus molle* and *Schinus Terebinthifolius*, *Evidence-Based Complementary Altern. Med*., 2022. doi: 10.1155/2022/4288890
35. J.S. Santana, P. Sartorelli, R.C. Guadagnin, A.L. Matsuo, C.R. Figueiredo, M.G. Soares, A.M. da Silva and J.H.G. Lago, Essential oils from *Schinus Terebinthifolius* leaves–chemical composition and *in vitro* cytotoxicity evaluation, *Pharm. Biol*., 2012, **50**, 1248–1253. doi: 10.3109/13880209.2012.666880
36. K. Chkirate, K. Azgaou, H. Elmsellem, B. El Ibrahimi, N.K. Sebbar, M. Benmessaoud, S. El Hajjaji and E.M. Essassi, Corrosion inhibition potential of 2-[(5-methylpyrazol-3-yl) methyl] benzimidazole against carbon steel corrosion in 1 M HCl solution: Combining experimental and theoretical studies, *J. Mol. Liq*., 2021, **321**, 114750. doi: 10.1016/j.molliq.2020.114750
37. A. Chraka, N.B. Seddik, I. Raissouni, J. Kassout, M. Choukairi, M. Ezzaki, O. Zaraali, H. Belcadi, F. Janoub and A.I. Mansour, Electrochemical explorations, SEM/EDX analysis, and quantum mechanics/molecular simulations studies of sustainable corrosion inhibitors on the Cu-Zn alloy in 3% NaCl solution, *J. Mol. Liq*., 2023, **387**, 122715. doi: 10.1016/j.molliq.2023.122715
38. K. Tassaoui, M. Damej, A. Molhi, A. Berisha, M. Errili, S. Ksama, V. Mehmeti, S. El Hajjaji and M. Benmessaoud, Contribution to the corrosion inhibition of Cu–30Ni copper–nickel alloy by 3-amino-1, 2, 4-triazole-5-thiol (ATT) in 3% NaCl solution. Experimental and theoretical study (DFT, MC and MD), *Int. J. Corros. Scale Inhib*., 2022, **11**, no. 1, 221–244. doi: 10.17675/2305-6894-2022-11-1-12
39. F. Bensabah, S. Houbairi, M. Essahli, A. Lamiri and J. Naja, Chemical composition and inhibitory effect of the essential oil from *Mentha Spicata* irrigated by wastewater on the corrosion of aluminum in 1 molar hydrochloric acid, *Electrochim. Acta*, 2013, **31**, 195–206. doi: 10.4152/pea.201304195

40. J. Chang, Z. Wang, E.-h. Han, X. Liang, G. Wang, Z. Yi and N. Li, Corrosion resistance of tannic acid, d-limonene and nano-ZrO_2 modified epoxy coatings in acid corrosion environments, *J. Mater. Sci. Technol*., 2021, **65**, 137–150. doi: 10.1016/j.jmst.2020.03.081
41. K.C. Oliveira, L.M.S.S. Franciscato, S.S. Mendes, F.M.A. Barizon, D.D. Gonçalves, L.N. Barbosa, M.G.I. Faria, J.S. Valle, R.F.A. Casalvara and J.E. Gonçalves, Essential Oil from the Leaves, Fruits and Twigs of *Schinus Terebinthifolius*: Chemical Composition, Antioxidant and Antibacterial Potential, *Molecules*, 2024, **29**, 469. doi: 10.3390/molecules29020469
42. A. Pawlowski, E. Kaltchuk-Santos, C.A. Zini, E.B. Caramão and G.L.G. Soares, Essential oils of *Schinus Terebinthifolius* and *S. molle* (*Anacardiaceae*): Mitodepressive and aneugenic inducers in onion and lettuce root meristems, *S. Afr. J. Bot*., 2012, **80**, 96–103. doi: 10.1016/j.sajb.2012.03.003
43. E. Todirascu-Ciornea, H.A.S. El-Nashar, N.M. Mostafa, O.A. Eldahshan, R.S. Boiangiu, G. Dumitru, L. Hritcu and A.N.B. Singab, *Schinus Terebinthifolius* essential oil attenuates scopolamine-induced memory deficits via cholinergic modulation and antioxidant properties in a zebrafish model, *Evidence-Based Complementary Altern. Med*., 2019. doi: 10.1155/2019/5256781
44. K.K.J. I.A. Annon, N. Betti, T.S. Gaaz, M.M. Hanoon, F.F. Sayyid, A.M. Mustafa and A.A. Alamiery., Unlocking corrosion defense: investigating Schiff base derivatives for enhanced mild steel protection in acidic environments, *Int. J. Corros. Scale Inhib*., 2024, **13**, no. 2, 727–749. doi: 10.17675/2305-6894-2024-13-2-5
45. A.E. Sultan, N.S. Abtan, F.F. Sayyid, A.A. Alamiery, A.H. Jaaz, T.S. Gaaz, S.M. Ahmed, A.M. Mustafa, D.A. Ali and M.M. Hanoon, Enhancing corrosion resistance of mild steel in hydrochloric acid solution using 4-phenyl-1-(phenylsulfonyl)-3-thiosemicarbazide: A comprehensive study, *Int. J. Corros. Scale Inhib*., 2024, **13**, no. 1, 435–459. doi: 10.17675/2305-6894-2024-13-1-22
46. Z.A. Gbashi, M.H. Abdulkareem, B.A. Abdulhussein, M.M. Hanoon, A.A.H. Kadhum, A.A. Alamiery and W.K. Al-Azzawi, Investigating the corrosion inhibitory properties of 1-benzyl-4-imidazolidinone on mild steel in hydrochloric acid: a thorough experimental and quantum chemical study., *Int. J. Corros. Scale Inhib*., 2024, **13**, no. 1, 411–434. doi: 10.17675/2305-6894-2024-13-1-21
47. O.A. Goncharova, A.Y. Luchkin, N.N. Andreev, N.P. Andreeva and S.S. Vesely, Triazole derivatives as chamber inhibitors of copper corrosion, *Int. J. Corros. Scale Inhib*., 2018, **7**, no. 4, 657–672. doi: 10.17675/2305-6894-2018-7-4-12
48. G. Palumbo, K. Berent, E. Proniewicz and J. Banaś, Guar gum as an eco-friendly corrosion inhibitor for pure aluminium in 1 M HCl solution, *Materials*, 2019, **12**, 2620. doi: 10.3390/ma12162620
49. X. Li and S. Deng, Synergistic inhibition effect of walnut green husk extract and potassium iodide on the corrosion of cold rolled steel in trichloroacetic acid solution, *J. Mater. Res. Technol*., 2020, **9**, 15604–15620. doi: 10.1016/j.jmrt.2020.11.018

50. R.S. Al-Moghrabi, A.M. Abdel-Gaber and H.T. Rahal, A comparative study on the inhibitive effect of *Crataegus oxyacantha* and *Prunus avium* plant leaf extracts on the corrosion of mild steel in hydrochloric acid solution, *Int. J. Ind. Chem*., 2018, **9**, 255–263. doi: 10.1007/s40090-018-0154-3
51. H.T. Rahal, A.M. Abdel-Gaber and R. Awad, Corrosion behavior of a superconductor with different SnO_2 nanoparticles in simulated seawater solution, *Chem. Eng. Commun*., 2017, **204**, 348–355. doi: 10.1080/00986445.2016.1271794
52. J. Zhou, S. Chen, L. Zhang, Y. Feng and H. Zhai, Studies of protection of self-assembled films by 2-mercapto-5-methyl-1, 3, 4-thiadiazole on iron surface in 0.1 M H_2SO_4 solutions, *J. Electroanal. Chem*., 2008, **612**, 257–268. doi: 10.1016/j.jelechem.2007.10.011
53. A.Y.I. Rubaye, A.A. Abdulwahid, S.B. Al-Baghdadi, A.A. Al-Amiery, A.A.H. Kadhum and A.B. Mohamad, Cheery sticks plant extract as a green corrosion inhibitor complemented with LC-EIS/MS spectroscopy, *Int. J. Electrochem. Sci*., 2015, **10**, 8200–8209. doi: 10.1016/S1452-3981(23)11087-X
54. M.V. Fiori-Bimbi, P.E. Alvarez, H. Vaca and C.A. Gervasi, Corrosion inhibition of mild steel in HCL solution by pectin, *Corros. Sci*., 2015, **92**, 192–199. doi: 10.1016/j.corsci.2014.12.002
55. G. Aziate, A. El Yadini, H. Saufi, A. Almaofari, A. Benhmama, H. Harhar, S. Gharby and S. El Hajjaji, Study of jojoba vegetable oil as inhibitor of carbon steel C38 corrosion in different acidic media, *J. Mater. Environ. Sci*., 2015, **6**, 1877–1884.
56. J. Du, C. Li, P. Liu, J. Liu, X. Chen, G. Wang, Z. Zuo, C. Huang, F. Lou and M. Wang, Inhibition effect of nano-silica synergistic corrosion inhibitor on 110SSsteel in ultra-high temperature organic acidic environment, *Corros. Eng., Sci. Technol*., 2023, **58**, 799–810. doi: 10.1080/1478422X.2023.2262215
57. T.A. Salman, A.A. Al-Amiery, L.M. Shaker, A. Kadhum and M.S. Takriff, A study on the inhibition of mild steel corrosion in hydrochloric acid environment by 4-methyl-2-(pyridin-3-yl) thiazole-5-carbohydrazide, *Int. J. Corros. Scale Inhib*., 2019, **8**, no. 4, 1035–1059. doi: 10.17675/2305-6894-2019-8-4-14

♦ ♦ ♦